Antonie van Leeuwenhoek (2013) 104:521–532
DOI 10.1007/s10482-013-9999-9

ORIGINAL PAPER

Crescent and star shapes of members of the *Chlamydiales* order: impact of fixative methods

Brigida Rusconi · Julia Lienard · Sébastien Aeby · Antony Croxatto · Claire Bertelli · Gilbert Greub

Received: 3 May 2013 / Accepted: 7 August 2013 / Published online: 14 August 2013

Abstract Members of the *Chlamydiales* order all share a biphasic lifecycle alternating between small infectious particles, the elementary bodies (EBs) and larger intracellular forms able to replicate, the reticulate bodies. Whereas the classical *Chlamydia* usually harbours round-shaped EBs, some members of the *Chlamydia*-related families display crescent and star-shaped morphologies by electron microscopy. To determine the impact of fixative methods on the shape of the bacterial cells, different buffer and fixative combinations were tested on purified EBs of *Criblamydia sequanensis*, *Estrella lausannensis*, *Parachlamydia acanthamoebae*, and *Waddlia chondrophila*. A linear discriminant analysis was performed on particle metrics extracted from electron microscopy images to recognize crescent, round, star and intermediary forms. Depending on the buffer and fixatives used, a mixture of alternative shapes were observed in varying proportions with stars and crescents being more frequent in *C. sequanensis* and *P. acanthamoebae*, respectively. No tested buffer and chemical fixative preserved ideally the round shape of a majority of bacteria and other methods such as deep-freezing and cryofixation should be applied. Although crescent and star shapes could represent a fixation artifact, they certainly point towards a diverse composition and organization of membrane proteins or intracellular structures rather than being a distinct developmental stage.

Keywords *Chlamydia* · Fixation · Electron microscopy · Ultrastructure

Brigida Rusconi and Julia Lienard have contributed equally to this study.

Electronic supplementary material The online version of this article (doi:10.1007/s10482-013-9999-9) contains supplementary material, which is available to authorized users.

B. Rusconi · J. Lienard · S. Aeby · A. Croxatto · C. Bertelli · G. Greub (✉)
Center for Research on Intracellular Bacteria, Institute of Microbiology, University Hospital Center and University of Lausanne, Rue du Bugnon 48, 1011 Lausanne, Switzerland
e-mail: gilbert.greub@chuv.ch

C. Bertelli
SIB Swiss Institute of Bioinformatics, Lausanne, Switzerland

Introduction

Chlamydiales, which belong to the *Chlamydiae* phylum of the *Planctomycetes*, *Verrucomicrobia*, *Chlamydia* (PVC) superphylum are obligate intracellular bacteria that have been isolated from a variety of clinical and environmental samples (Lienard and Greub 2011; Horn 2008). The term *Chlamydia*-related bacteria has been used to coin a variety of bacterial species that belong to several families phylogenetically related to the well-known pathogens *Chlamydia*.

These bacteria have the ability to infect a wide range of hosts and cell lines, some being able to grow within amoebae (Greub and Raoult 2004; Corsaro et al. 2009), human cell lines (Goy et al. 2008; Kebbi-Beghdadi et al. 2011b), arthropods (Corsaro et al. 2007) or fishes (Kebbi-Beghdadi et al. 2011a). However, members of the *Chlamydiales* all share a unique life cycle. Their infectious elementary body (EB) is internalized into the host cell within a membrane-bound vacuole termed an inclusion. Soon after entry, the EB differentiates into a reticulate body (RB) and divides by binary fission. Finally, RBs re-differentiate into EBs and lyse the host cell to start a new infection cycle.

Chlamydiaceae usually harbour round-shaped EBs that are small in size (0.3–0.35 μm) as well as slightly larger RBs (0.5–2.0 μm) (Mitchell et al. 2009; Miyashita et al. 2001). These round shapes were confirmed by freeze deep-etching (Matsumoto et al. 1976). The *Chlamydiales* do not encode for a complete set of genes for the cell wall synthesis (McCoy and Maurelli 2006). It is therefore believed that the structure of the bacteria is given by the network of cysteine-rich membrane proteins. During the past decade, particular EB cell morphologies were described for new members of the *Chlamydiales* order. An electron micrograph study of *Parachlamydia acanthamoebae* in the amoeba *Acanthamoeba polyphaga* showed the occurrence of crescent shapes mainly within amoebal inclusions (Greub and Raoult 2002). This latter form, also seen with other members of the *Parachlamydiaceae* family (Amann et al. 1997; Horn et al. 2000), was proposed as a potential third replicative stage. This stage exhibits similar biological characteristics to EBs, being an infectious stage that enters in amoebae passively by phagocytosis and that accumulates in vacuoles full of EBs at late time points (Greub and Raoult 2002). Crescent bodies are estimated to be of the same size as EBs (0.5 μm large), while RBs are about 0.6 μm large.

Subsequently, a new chlamydial species called *Criblamydia sequanensis* was discovered using amoebal co-culture of a water sample from the Seine river (Thomas et al. 2006). This bacterium exhibited an unusual star-shaped EB and an oblong lamellar structure within its cytoplasm. Recently, *Estrella lausannensis* was described as a new species harbouring similar phenotypic characteristics, except for the absence of the translucent lamellar structure (Lienard et al. 2011). The star-shaped morphology of EBs of *C. sequanensis* and *E. lausannensis* was proposed as a distinctive characteristic of the *Criblamydiaceae* family (Lienard et al. 2011). As for *Parachlamydia*, EBs were shown to be slightly smaller than RBs, with sizes ranging between 0.5–1 and 0.8–1.8 μm, respectively. The crescent and star shapes might also appear following use of fixative and buffer during the preparation of the embedded electron microscopy samples. This hypothesis was previously described in a report by Lindsay et al. (1995) on the impact of fixative and buffer on *Planctomycetes* morphology. In this study the authors describe the presence of crescent-shaped *Planctomycetes* upon fixation with certain buffer and fixative combinations.

In this contribution, we show the effect of different fixation methods for electron microscopy on the morphology of four bacteria across three different families of the *Chlamydiales* order: *Waddliaceae*, *Parachlamydiaceae*, and *Criblamydiaceae*. We establish that the proportion of crescent and star shapes are dependent on fixatives and buffers used for sample preparation. These shapes probably do not correspond to additional developmental stages but are more likely to reflect differences in the underlying bacterial membrane protein composition or organization.

Materials and methods

Strains

The following bacterial strains were used: *Waddlia chondrophila* (ATCC VR-1470), *C. sequanensis* (CRIB18), *P. acanthamoebae* (Hall's *coccus*), and *E. lausannensis* (CRIB30). These bacteria were propagated in *Acanthamoeba castellanii* (ATCC30010).

Preparation of purified elementary bodies

The following fixation conditions were tested on EBs purified as previously described (Greub et al. 2003b). Briefly, bacteria were produced by infection of *A. castellanii*. Lysed culture was centrifuged at 180×*g* to remove amoebal debris. Then bacteria were pelleted at 6,600 g. Bacteria were washed in a PBS, 10 % sucrose solution and centrifuged as previously reported (Greub et al. 2003a). The EBs were then separated by ultracentrifugation with a discontinuous

gastrographin gradient. Purified bacteria were stored frozen at −80 °C in 10 % glycerol in PBS or succinic, phosphate, glycine (SPG) buffer prior to fixation. One or two vials of frozen bacteria (1 ml) were thawed and centrifuged for 10 min at 7,500×*g*. Bacteria were washed with 3 mM Hepes and split in two samples prior to centrifugation. Pellets were resuspended in 300 µl of 100 mM PBS or 3 mM Hepes. The samples were centrifuged again and resuspended in the same buffers. The samples resuspended in 3 mM Hepes were used for the two Hepes conditions (3 and 100 mM). After overnight fixation of all the samples with the corresponding fixative (1 % osmium tetroxide or 3 % glutaraldehyde) at 4 °C, the samples were washed three times with the corresponding buffer: 3 mM or 100 mM Hepes or 100 mM PBS. After a PBS wash, cells were further fixed with 1 % osmium tetroxide in PBS for 1 h at room temperature. Samples were dehydrated with subsequent increasing ethanol washes (50–100 %). Samples were then transferred into propylene oxide and incubated over night in an epoxy resin (Epon) mixed with 50 % propylene oxide as described previously (Casson et al. 2006). Samples were embedded in agar capsules. Thin sections obtained with the LKB 2088 Ultrotome were deposited on formvar coated copper grids and stained. Sections were stained with methanol-uranyl acetate and lead nitrate with sodium citrate for 10 min. Sections were acquired with a transmission electron microscope with a 80 kV filament (Philips EM 201). Thus, a total of 6 conditions were investigated, i.e. 3 buffers (100 mM Hepes, 3 mM Hepes, 100 mM PBS) and two different fixatives (1 % osmium tetroxide, 3 % glutaraldehyde). Osmolarity of the different buffers can be found in Supplementary Table S1. The osmolarity was measured with a 2020 Osmometer from Applied Instruments (Vlissingen, The Netherlands).

Image analysis

Electron microscopy images of EBs taken at 7,000× magnification were transformed in a mask with the function "Make Binary" of ImageJ (Schneider et al. 2012; Rasband 1997–2012). The images were further analyzed with the "Analyze Particle" plugin to extract a set of parametric values (Supplementary Table S2; Fig. S1) that characterize each particle. To exclude potentially remaining RBs and aberrant forms, particles outside the following circularity and size cutoff were excluded (Circularity: 0.2–1, size: 0.02–0.15 pixel^2). To control for bacterial aggregation problems the mean area was determined by quantifying the mean particle size in images without size filter.

To identify the combination of ideally discriminating parameters for each type of shapes (crescent, star, convex polygon, round, undetermined large, undetermined small), a set of 488 particles was visually and manually selected. Each particle was assigned randomly to a training set (200 particles) or to a test set (288 particles), implying that training and test sets are non-redundant. A linear discriminant analysis (LDA) was trained on the training set. Then, the LDA was used to predict the shape of the test set allowing to measure the accuracy of shape assignment. Finally, each picture was automatically processed through ImageJ and LDA analysis respectively to evaluate the proportion of each shape. During the LDA analysis, all objects recognized as a valid particle by ImageJ were classified in either one of the shapes.

In addition, to assess the global performance of LDA on varying training sets, 100 random training sets and their complementary test sets were used to train 100 LDA and determine in each case the specificity and sensitivity of shape assignment. LDA analyses were performed using R (RCoreTeam 2012) and package MASS (Venables and Ripley 2002).

Statistical analysis

Statistical analysis of morphology quantification was performed with GraphPad Prism v6.0 (GraphPad, LaJolla, USA). Unpaired t-tests with Welch's correction were conducted on all results to determine significant differences of shape distribution. Correlations were calculated using the Pearson correlation coefficient.

Results

Computer-based determination of bacterial morphology

In the *Chlamydiales* order several different morphologies were previously described (Greub and Raoult 2002; Lienard et al. 2011; Thomas et al. 2006; Corsaro et al. 2007). We investigated the role of two fixatives and three buffers chosen accordingly to Lindsay et al.

1995 on the morphology of 4 *Chlamydia*-related species *C. sequanensis*, *E. lausannensis* (*Criblamydiaceae*), *W. chondrophila* (*Waddliaceae*), and *P. acanthamoebae* (*Parachlamydiaceae*) (Table 1). In our study we defined the following shapes: crescent, star, convex polygon, round, undetermined large and undetermined small (Fig. 1a). The undetermined small shape generally corresponded to small EBs with an irregular shape or bacterial debris. The large undetermined shapes were often constituted of two bacteria too close to each other to allow distinct outline recognition.

Determination of bacterial morphological features by computer-assisted analysis of images has proven to be quite challenging. The human eye has a very unique ability to readily and reliably detect different complex shapes within a picture. A collection of shapes selected by eye were used to define finite parameters for computer-based analysis that allow the automated classification of each particle within any picture to each shape.

Thirteen parameters that define different metrics of particle shape and size for each pre-determined population were acquired. Simple combinations of two parameters were not sufficient to discriminate between all shapes (Fig. 1b, Supplementary Fig. S1). Therefore, we performed a LDA that attempts to express the shape category as a linear combination of all available parameters (Fig. 1c). The LDA was trained on a set of 200 manually selected particles and then tested against a different set of 288 particles to assess the accuracy of shape classification (Table 2). An analysis of 100 random training sets and the 100 complementary test sets among the 488 particles manually selected achieved a mean specificity above 96 % and a mean sensitivity ranging between 75 % for crescent shape and 97 % for round shape (Fig. 1d).

Effect of fixatives and buffers on the number of particle analyzed

Including all fixative and buffer conditions tested, we analyzed a total of 91,062 particles. The sample density was low enough to allow recognition of different shapes in each buffer and fixative conditions. For *C. sequanensis* and *E. lausannensis*, fixation with 3 % glutaraldehyde and 100 mM Hepes caused a severe lysis of the bacteria that did not allow the acquisition of enough particles for analysis (Table 1). The same lysis occurred with *P. acanthamoebae* in 3 % glutaraldehyde 100 mM PBS (Supplementary Fig. S3). To rule out that aggregation of bacteria significantly leads to a reduced number of particles counted, we quantified the mean particle area for each condition (Supplementary Fig. S2). For none of the bacteria, we could observe a correlation between the mean area and the initial bacterial concentration. However, for *W. chondrophila* and *C. sequanensis* the area was significantly higher for 100 mM PBS in 1 % osmium tetroxide compared to all other investigated conditions (Fig. S2).

To investigate the role of the fixative on the preservation of bacterial cells, the number of bacteria present in each sample was determined by normalizing the number of particles acquired with the number of images taken and the dilution of bacteria used for fixation (Fig. 2a). For all buffer conditions except one, significantly ($p < 0.0001$) more EBs were observed with 3 % glutaraldehyde compared to 1 % osmium tetroxide. Only for *P. acanthamoebae* 100 mM Hepes there were more particles with 1 % osmimum tetroxide ($p < 0.0001$). Subsequently, despite the higher proportion of particles acquired in 3 % glutaraldehyde, one condition was causing the complete lysis of EBs in three out of four bacteria. Therefore, we

Table 1 Particles acquired per condition and bacterial species

Species	3 % glutaraldehyde			1 % osmium tetroxide		
	100 mM Hepes	3 mM Hepes	100 mM PBS	100 mM Hepes	3 mM Hepes	100 mM PBS
C. sequanensis	NA	7,600	5,306	6,365	6,960	5,663
E. lausannensis	NA	1,497	734	1,087	2,518	1,160
W. chondrophila	8,331	6,805	6,477	5,095	4,169	4,568
P. acanthamoebae	2,584	2,675	NA	4,615	4,095	2,758
Total	10,925	18,577	12,517	17,162	17,742	14,149

NA not analyzed

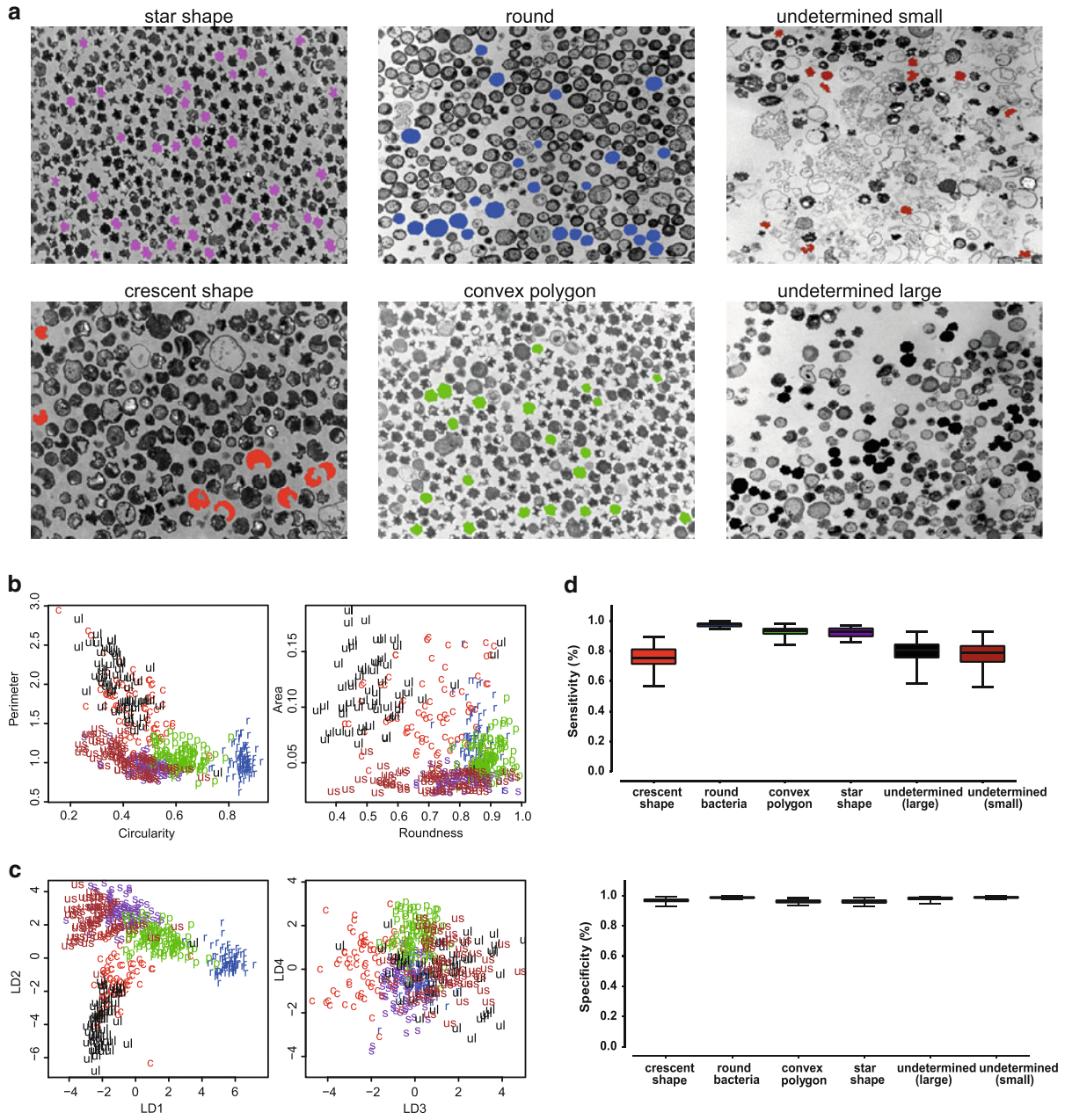

Fig. 1 Method for quantification of morphological features of bacteria. **a** Reference shapes were selected by eye and their parameters acquired with ImageJ. Magnification of ×7,000. **b** Two parameters do not allow a good discrimination of shapes. **c** Combination of parameters by the linear discriminant analysis is optimized to separate the different shapes. **d** Sensitivity and specificity of LDA predictions based on 100 random training and each complementary test datasets. *Color code* of figure: crescent *red*, star *purple*, round *blue*, convex polygon *green*, undetermined small *brown*, undetermined large *black*. Undetermined small represent small EBs without defined shape or bacterial debris. Undetermined big represent two EBs too close to allow separate recognition by ImageJ

determined the influence of the buffer on the lysis of the bacteria in 1 % osmium tetroxide fixed cells (Fig. 2a). Again, the percentage was calculated as the number of particles normalized by the number of images acquired and the dilution of the sample. For all bacteria there were significantly more particles

Table 2 Confusion table of specificity and sensibility

Shape	True positive	False positive	True negative	False negative	Sensitivity	Specificity
Crescent	35	9	235	9	79.5	96.3
Round	51	1	234	2	96.2	99.6
Convex polygon	57	5	226	0	100	97.8
Star	54	8	223	3	94.7	96.5
Undetermined large	34	3	244	7	82.9	98.8
Undetermined small	28	3	249	8	77.8	98.8

analyzed with 100 mM PBS compared to 100 mM Hepes ($p < 0.0001$) and with 3 mM Hepes compared to 100 mM Hepes ($p < 0.0001$). When comparing 100 mM PBS to 3 mM Hepes the percentage of particles was still significantly higher with 100 mM PBS for *C. sequanensis* ($p < 0.0001$), *W. chondrophila* ($p < 0.0001$), and *P. acanthamoebae* ($p < 0.02$). Overall, the 100 mM PBS buffer appeared to better preserve the bacteria.

Effect of fixatives and buffers on bacterial morphology

The LDA allowed us to quantify for each fixation the amount of each bacterial shape (Fig. 2b). In a first step, we determined the effect of the fixative on the proportion of different shapes by comparing the same buffer, when applicable (Table 3). For *P. acanthamoebae*, fixation with 1 % osmium tetroxide with 3 mM Hepes or 100 mM Hepes reduced the number of crescent bodies compared to 3 % glutaraldehyde. On the other hand, for the same buffer *W. chondrophila* showed an increase ($p < 0.0001$) in crescent shapes with the 1 % osmium tetroxide fixation. For the phosphate buffer (100 mM PBS) only *C. sequanensis* exhibited a significant decrease ($p = 0.0005$) of crescent shapes with the 1 % osmium tetroxide fixation. In summary depending on the bacterial species, an increase or decrease in the number of crescent shapes was observed with the different fixatives.

We saw an increase in star shapes with 3 mM Hepes/1 % osmium tetroxide compared to 3 % glutaraldehyde for *E. lausannensis* ($p < 0.0001$) and *W. chondrophila* ($p < 0.0001$). In contrast, *C. sequanensis* ($p < 0.0001$) and *P. acanthamoebae* ($p = 0.0097$) presented a decreased proportion of star shapes in the same conditions (Table 3). Overall, we observed fewer star shapes with 1 % osmium tetroxide.

When comparing fixatives for round-shaped bacteria a decrease with both 3 mM Hepes/1 % osmium tetroxide ($p < 0.0001$) and 100 mM PBS/osmium tetroxide ($p < 0.0001$) was observed for *C. sequanensis* compared to 3 % glutaraldehyde. For *E. lausannensis* ($p = 0.0003$) and *W. chondrophila* ($p < 0.0001$), we also observed a reduced proportion of round-shaped bacteria with 3 mM Hepes/1 % osmium tetroxide and 100 mM Hepes/1 % osmium tetroxide, respectively. Only for *P. acanthamoebae* an increase in round-shaped bacteria with both 3 and 100 mM Hepes/1 % osmium tetroxide ($p < 0.0001$) was observed (Table 3). In summary, we again observed different changes in shapes depending on the bacterial species.

The second aim of our study was to determine the role of the different buffers on the morphology of the bacteria. The percentage of crescent-, star-, and round-shaped bacteria fixed with 1 % osmium tetroxide according to the buffer used was determined (Fig. 2b). For *C. sequanensis* and *W. chondrophila* no significant change in the proportion of crescent shapes was observed with the three different buffers. For *P. acanthamoebae* there were more crescent-shaped bacteria in 100 mM PBS compared to both 100 mM Hepes ($p < 0.0001$) and 3 mM Hepes ($p < 0.0001$). For *P. acanthamoebae* the change in buffer rather than the change in concentration affected the proportion of crescent-shaped bacteria (Table 3).

The proportion of star shapes were strongly associated with the use of an Hepes buffer, star shapes being present in lower numbers in 100 mM PBS than in any concentration of Hepes buffer (Table 3). For all except *P. acanthamoebae* more round-shaped bacteria were observed in 100 mM PBS compared to both 3 and 100 mM Hepes (Table 3). In summary, 100 mM PBS reduced the proportion of star shapes in favour of more round-shaped bacteria. In general, the proportion of crescent-, star- and round-shaped *C. sequanensis*,

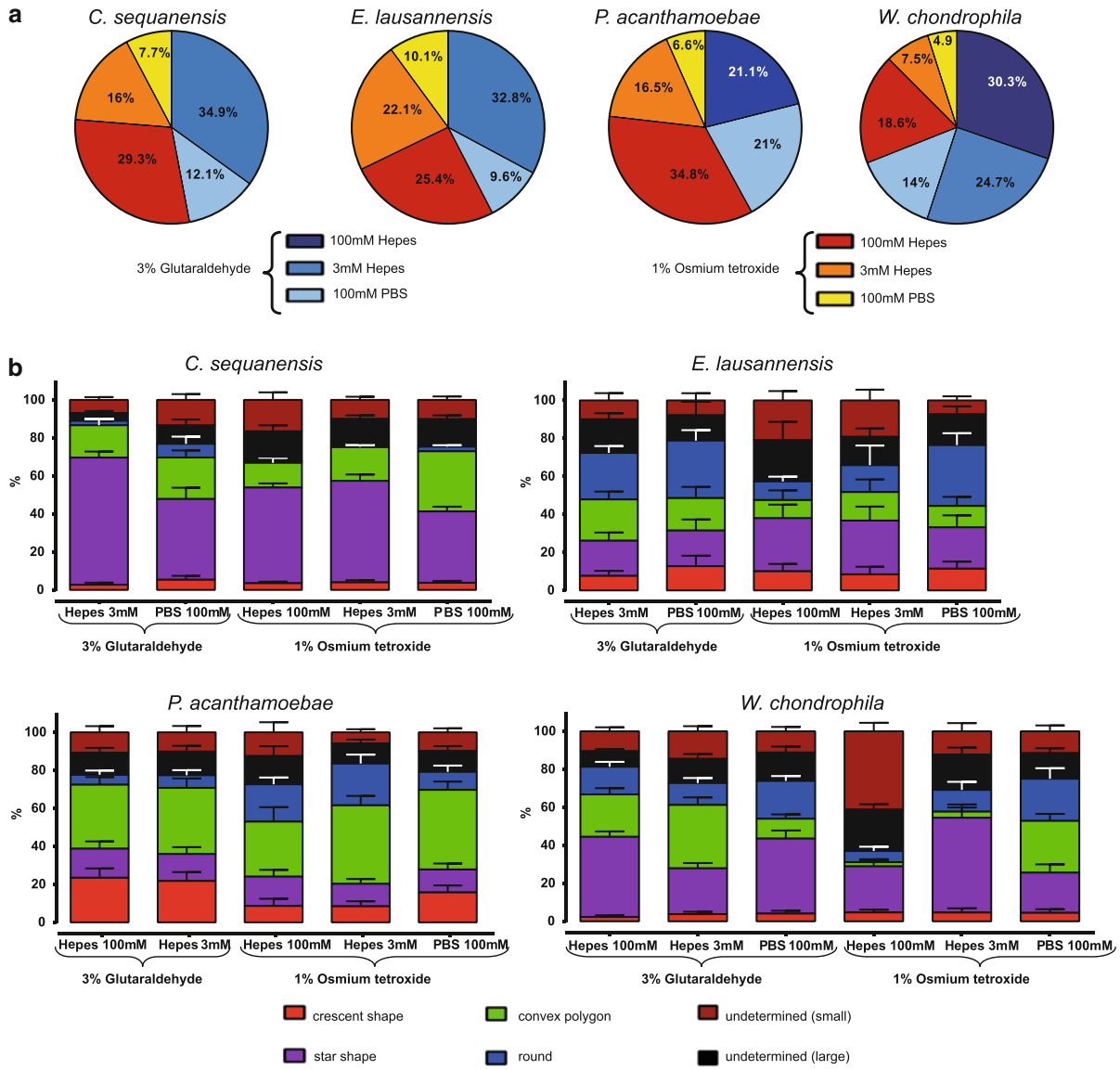

Fig. 2 Quantification of bacterial morphological features depending on fixation. **a** Percentage of bacteria in sample per fixation condition. The proportion of elementary bodies (EBs) detected in each fixation and buffer condition was compared to the total amount of EBs quantified for each bacterium. A lower concentration of bacteria was observed with 1 % osmium tetroxide in almost all bacteria. **b** For each bacterium the percentage of each *shape* is represented according to fixation method (compared to the total amount of EBs for each condition and bacteria)

W. chondrophila, and *E. lausannensis* changed in the same way when comparing different buffers. *P. acanthamoebae* on the other hand often showed an opposite behavior, i.e. a decrease of round-shaped bacteria with 100 mM PBS compared to 100 mM Hepes. Still, 100 mM PBS appeared to be the best buffer, since the proportion of undetermined shapes was low for all bacteria in this condition (Fig. 2b). Conversely, the 100 mM Hepes, 1 % osmium tetroxide combination increased strongly the proportion of undetermined shapes for all four species.

Considering 100 mM PBS with 1 % osmium tetroxide to be the least aggressive and best preserving fixative we then compared the percentage of crescent, star and round shapes between different species. In this condition *P. acanthamoebae* presented the highest

Table 3 Effect of fixatives and buffers on the percentage of each shape observed

			1 % osmium tetroxide		
			3 mM Hepes	100 mM Hepes	100 mM PBS
Crescent shapes	*P. acanthamoebae*	3 mM Hepes	−−−−	ns	−−−−−
		100 mM Hepes		−−−−	−−−−−
		100 mM PBS			NA
	W. chondrophila	3 mM Hepes	ns	ns	ns
		100 mM Hepes		++++	ns
		100 mM PBS			ns
	C. sequanensis	3 mM Hepes	+++	ns	ns
		100 mM Hepes		NA	ns
		100 mM PBS			−−−
	E. lausannensis	3 mM Hepes	ns	ns	−
		100 mM Hepes		NA	ns
		100 mM PBS			ns
Star shapes	*P. acanthamoebae*	3 mM Hepes	−−	−−−	ns
		100 mM Hepes		ns	+++
		100 mM PBS			NA
	W. chondrophila	3 mM Hepes	++++	++++	++++
		100 mM Hepes		−−−−	++
		100 mM PBS			−−−−
	C. sequanensis	3 mM Hepes	−−−−	+++	++++
		100 mM Hepes		NA	++++
		100 mM PBS			−−−
	E. lausannensis	3 mM Hepes	++++	ns	+
		100 mM Hepes		NA	+
		100 mM PBS			ns
Round shapes	*P. acanthamoebae*	3 mM Hepes	++++	+	++++
		100 mM Hepes		++++	++++
		100 mM PBS			NA
	W. chondrophila	3 mM Hepes	ns	++++	−−−−−
		100 mM Hepes		−−−−	−−−−−
		100 mM PBS			ns
	C. sequanensis	3 mM Hepes	−−−−	ns	−−−−−
		100 mM Hepes		NA	−−−−−
		100 mM PBS			−−−−
	E. lausannensis	3 mM Hepes	−−−	ns	−−−−−
		100 mM Hepes		NA	−−−−−
		100 mM PBS			ns

Comparison between fixatives in diagonal (±compared to gluataraldehyde). Comparison between buffer in 1 % osmium tetroxide (±compared to buffer in the same column)

NA not analyzed, *ns* not significant

$+/-p < 0.05$; $++/--p < 0.01$; $+++/---p < 0.001$; $++++/----p < 0.0001$

percentage (15.8 %) of crescent shapes, followed by *E. lausannensis*, *W. chondrophila* and *C. sequanensis* that harboured less than 5 % crescent shapes. More than a third (37.5 %) of *C. sequanensis* particles were star-shaped, followed by *E. lausannensis* and *W. chondrophila* at about 20 % and finally *P. acanthamoebae*

that presented only 12 % star shapes. The highest proportion (32 %) of round-shaped bacteria was found in *E. lausannensis* followed by *W. chondrophila* (22 %), *P. acanthamoebae* (9.5 %) and finally *C. sequanensis* (2.4 %). In summary, under these fixation and buffer conditions, *C. sequanensis* is mainly characterized by star shapes, *E. lausannensis* by round-shaped bacteria, *P. acanthamoebae* by crescent and convex polygons, while *W. chondrophila* had an equal proportion of star, round and convex polygon particles.

Discussion

Morphology of bacteria is strongly dependent on the composition of the cellular membrane and the cell wall. Bacteria with a peptidoglycan display a higher rigidity, preventing significant changes in cell shape and size. Members of the PVC superphylum encode genes for peptidoglycan biosynthesis to a varying degree (Labutti et al. 2010; Stephens et al. 1998; Yoon et al. 2010). According to a post-genomic analysis of peptidoglycan biosynthesis based on three necessary genes (GT28, GT51, one of five GH family genes) both *Chlamydiales* and *Planctomycetes* do not synthesize peptidoglycan (Cayrou et al. 2012). Indeed, so far no peptidoglycan was ever isolated from *Planctomycetes* and *Chlamydiae* (Fox et al. 1990; Yoon et al. 2010). Still, for *Chlamydia pneumoniae* the peptidoglycan precursor lipid II was produced by chlamydial proteins (MraY, MurG) from the substrate UDP-MurNAc-pentapeptide in vitro (Henrichfreise et al. 2009). Moreover, *Chlamydiales* and some members of the *Planctomycetes* encode for penicillin binding protein homologs that might replace the missing transpeptidase function of GT51. The role of this peptidoglycan precursor in chlamydial cell wall organization remains controversial.

In this study we investigated the effect of different fixatives and buffers on the cell shape of these peptidoglycan-less bacteria in the phylum *Chlamydiae*. Confocal microscopy of cells infected with *W. chondrophila*, *P. acanthamoebae*, or *E. lausannensis* and labeled with fluorescent antibodies, generally display round bacteria (Goy et al. 2008; Greub et al. 2005; Lienard et al. 2011), but crescent bodies have been observed following paraformaldehyde fixation of *P. acanthamoebae* (Greub et al. 2005). Bacteria were stored frozen at −80 °C with 10 % glycerol or in SPG prior to fixation. Although we cannot exclude that this step might influence the morphology of the bacteria, the bacteria are viable and infectious. Using different chemical fixations, we could observe a different proportion of shapes, including crescents and stars, for all bacteria analyzed. Interestingly, the peptide cross-linking agent glutaraldehyde caused a higher lysis of the bacteria than the oxidizing osmium tetroxide in combination with higher osmolarity buffers (100 mM Hepes, 100 mM PBS). Moreover, round-shaped bacteria were more frequently observed with osmium tetroxide.

Even though Hepes 100 mM is considered to have an appropriate osmolarity range for natural shape conservation (Lindsay et al. 1995) for electron microscopy we observed that PBS preserved better the round shape for our bacteria. On the other hand, *P. acanthamoebae* 3 mM Hepes/1 % osmium tetroxide fixation resulted in more round-shaped bacteria than the other two buffers. For *C. sequanensis* none of the used fixatives or buffers resulted in more than 7 % of round-shaped bacteria. Other buffer conditions, like cacodylate should be tested to determine a buffer with appropriate osmolarity. Rather than osmolarity the ion composition might influence *C. sequanensis* morphology by electrostatic interactions with the cell wall.

In *Gemmata obscuriglobus* (*Planctomycetes*) the combination of 3 % glutaraldehyde and 3 mM Hepes increased the amount of crescent-shaped bacteria detected compared to 1 % osmium tetroxide (Lindsay et al. 1995). The same observation was made with *P. acanthamoebae* that showed the highest percentage of crescent shapes among the bacteria tested. Moreover, as with *G. obscuriglobus* an increase in osmolarity to 100 mM Hepes with 3 % glutaraldehyde increased the proportion of crescent shapes observed in *P. acanthamoebae*, although not to the same extent. This suggests that for *P. acanthamoebae* the fixative may play a major role in shape determination, probably influencing the membrane protein crosslinking. Glutaraldehyde could cause the crosslinking of the proteinaceous cell membrane to internal cell structures of *P. acanthamoebae* therefore increasing the alteration of bacterial morphology into crescent-shaped bacteria. This is also supported by the higher proportion of round bacteria with 1 % osmium tetroxide compared to 3 % glutaraldehyde with both Hepes buffer concentrations.

The formation of star shapes in *C. sequanensis* and crescent shapes in *P. acanthamoebae* is certainly triggered by some intrinsic differences in the membrane or proteinaceous layer of these bacteria. The different morphology of *Chlamydia*-related bacteria with the same fixative condition underlines the differences in membrane proteins determined by genome analysis (Bertelli et al. 2010; Horn et al. 2004) and proteomics (Heinz et al. 2010, 2009; Lienard et al. unpublished).

Presence and abundance of MOMP-like proteins varies significantly between *Chlamydia*-related bacteria, ranging from none in *Protochlamydia* to 35 in *Simkania negevensis* (Collingro et al. 2011). *W. chondrophila* and the two members of the *Criblamydiaceae* encode for about a dozen MOMP-like proteins. All bacteria analyzed in this paper encode for the large cysteine-rich outer membrane protein (OmcB), as well as an OmcA homolog. As mentioned by Collingro et al. (2011), *omcA* genes cannot be detected by simple homology searches. However, we were able to detect an *omcA* homolog by screening the upstream sequence of *omcB* for ORFs. Moreover, the polymorphic membrane protein family is strongly reduced in *W. chondrophila*, *Protochlamydia amoebophila* and *S. negevensis* (Collingro et al. 2011; Bertelli et al. 2010) as well as in *E. lausannensis* ($n = 1$) and in *C. sequanensis* ($n = 2$) compared to *Chlamydiaceae*. These differences in protein composition might partially explain the differences in cell shape observed for each species with the different fixatives. Uneven protein distribution combined with a reduced cross-linking of proteins by the fixative within the membrane may well result in "collapsing" parts. Finally, we cannot exclude the cross-linking of intracellular protein structures that are unevenly distributed inside the bacteria and could cause particular cellular shapes.

In summary, we observed that particular crescent and star shapes are observed in all *Chlamydia*-related species. Therefore, if only chemical fixations are used, presence of a given shape in any new isolate should be interpreted with caution to classify at the family level, and other criteria such as gene sequences should be used for taxonomy (Greub 2010). However, differences in the proportion of chlamydial cell shape depend on the species, fixatives, and buffers. While we consider the possibility that these shapes are artifacts the different patterns of morphologies certainly seem to be consistent with differences in the composition and the organization of the proteinaceous layer and membrane between different *Chlamydia*-related bacteria. Unusual morphologies have been described in other bacteria. Among others, cryofixed *Verrucomicrobia* present an elongated shape and spikes (Lee et al. 2009). Star-shaped bacteria were also observed by phase-contrast and electron microscopy of freshwater samples (Staley 1968). However, the exact nature of these bacteria is not known since they were observed in a mixed culture from a river isolate. It is so far not possible to link this to the presence/absence of known outer membrane proteins. For each new *Chlamydia*-related bacterium the chemical fixation must be optimized to preserve as much as possible the natural shape of the bacteria. The occurrence of these unusual shapes of EBs should be investigated using cryofixation or deep-freezing methods that ideally preserve bacterial integrity. Only these techniques will allow to determine if these shapes are actually present in the natural state or induced by chemical fixation. However, biosafety issues will still require a mild fixation step prior to cryofixation to prevent dissemination of infectious EBs.

Acknowledgments This work was supported by the Swiss National Science Foundation (project no. PDFMP3-127302). Brigida Rusconi is supported by the Swiss National Science Foundation within the PRODOC program "Infection and Immunity". Julia Lienard is supported by SUEZ-Environment (CIRSEE, Paris, France). We thank D. Bardy (CHUV) for measurements of osmolarity. We thank the PFMU at the Medical Faculty of Geneva for assisting with electron microscopy.

Conflict of interest The funders had no role in study design, data collection and analysis, decision to publish, or preparation of the manuscript. The authors declare having no conflict of interest related to the content of this contribution.

References

Amann R, Springer N, Schonhuber W, Ludwig W, Schmid EN, Muller KD, Michel R (1997) Obligate intracellular bacterial parasites of acanthamoebae related to *Chlamydia* spp. Appl Environ Microbiol 63(1):115–121

Bertelli C, Collyn F, Croxatto A, Rückert C, Polkinghorne A, Kebbi-Beghdadi C, Goesmann A, Vaughan L, Greub G (2010) The Waddlia genome: a window into chlamydial biology. PLoS ONE 5(5):e10890. doi:10.1371/journal.pone.0010890

Casson N, Medico N, Bille J, Greub G (2006) *Parachlamydia acanthamoebae* enters and multiplies within pneumocytes and lung fibroblasts. Microbes Infect 8(5):1294–1300. doi:10.1016/j.micinf.2005.12.011

Cayrou C, Henrissat B, Gouret P, Pontarotti P, Drancourt M (2012) Peptidoglycan: a post-genomic analysis. BMC Microbiol 12:294

Collingro A, Tischler P, Weinmaier T, Penz T, Heinz E, Brunham RC, Read TD, Bavoil PM, Sachse K, Kahane S, Friedman MG, Rattei T, Myers GSA, Horn M (2011) Unity in variety—the pan-genome of the Chlamydiae. Mol Biol Evol 28(12):3253–3270. doi:10.1093/molbev/msr161

Corsaro D, Thomas V, Goy G, Venditti D, Radek R, Greub G (2007) 'Candidatus Rhabdochlamydia crassificans', an intracellular bacterial pathogen of the cockroach Blatta orientalis (Insecta: Blattodea). Syst Appl Microbiol 30(3):221–228. doi:10.1016/j.syapm.2006.06.001

Corsaro D, Feroldi V, Saucedo G, Ribas F, Loret JF, Greub G (2009) Novel Chlamydiales strains isolated from a water treatment plant. Environ Microbiol 11(1):188–200

Fox A, Rogers JC, Gilbart J, Morgan S, Davis CH, Knight S, Wyrick PB (1990) Muramic acid is not detectable in *Chlamydia psittaci* or *Chlamydia trachomatis* by gas chromatography-mass spectrometry. Infect Immun 58(3): 835–837

Goy G, Croxatto A, Greub G (2008) *Waddlia chondrophila* enters and multiplies within human macrophages. Microbes Infect 10(5):556–562. doi:10.1016/j.micinf.2008.02.003

Greub G (2010) International committee on systematics of prokaryotes. Subcommittee on the taxonomy of the Chlamydiae: minutes of the closed meeting, 21 June 2010, Hof bei Salzburg, Austria. Int J Syst Evol Microbiol 60(Pt 11):2694. doi:10.1099/ijs.0.028233-0

Greub G, Raoult D (2002) Crescent bodies of *Parachlamydia acanthamoeba* and its life cycle within *Acanthamoeba polyphaga*: an electron micrograph study. Appl Environ Microbiol 68(6):3076–3084

Greub G, Raoult D (2004) Microorganisms resistant to free-living amoebae. Clin Microbiol Rev 17(2):413–433

Greub G, La Scola B, Raoult D (2003a) Parachlamydia acanthamoeba is endosymbiotic or lytic for *Acanthamoeba polyphaga* depending on the incubation temperature. Ann NY Acad Sci 990:628–634

Greub G, Mege J-L, Raoult D (2003b) *Parachlamydia acanthamoebae* enters and multiplies within human macrophages and induces their apoptosis. Infect Immun 71(10):5979–5985

Greub G, Mege J-L, Gorvel J-P, Raoult D, Méresse S (2005) Intracellular trafficking of *Parachlamydia acanthamoebae*. Cell Microbiol 7(4):581–589. doi:10.1111/j.1462-5822.2004.00488.x

Heinz E, Tischler P, Rattei T, Myers G, Wagner M, Horn M (2009) Comprehensive in silico prediction and analysis of chlamydial outer membrane proteins reflects evolution and life style of the Chlamydiae. BMC Genomics 10:634. doi:10.1186/1471-2164-10-634

Heinz E, Pichler P, Heinz C, Op Den Camp HJM, Toenshoff ER, Ammerer G, Mechtler K, Wagner M, Horn M (2010) Proteomic analysis of the outer membrane of *Protochlamydia amoebophila* elementary bodies. Proteomics 10(24):4363–4376. doi:10.1002/pmic.201000302

Henrichfreise B, Schiefer A, Schneider T, Nzukou E, Poellinger C, Hoffmann TJ, Johnston KL, Moelleken K, Wiedemann I, Pfarr K, Hoerauf A, Sahl HG (2009) Functional conservation of the lipid II biosynthesis pathway in the cell wall-less bacteria Chlamydia and Wolbachia: why is lipid II needed? Mol Microbiol 73(5):913–923

Horn M (2008) Chlamydiae as symbionts in eukaryotes. Annu Rev Microbiol 62:113–131. doi:10.1146/annurev.micro.62.081307.162818

Horn M, Wagner M, Muller KD, Schmid EN, Fritsche TR, Schleifer KH, Michel R (2000) *Neochlamydia hartmannellae* gen. nov., sp. nov. (Parachlamydiaceae), an endoparasite of the amoeba *Hartmannella vermiformis*. Microbiology 146(Pt 5):1231–1239

Horn M, Collingro A, Schmitz-Esser S, Beier CL, Purkhold U, Fartmann B, Brandt P, Nyakatura GJ, Droege M, Frishman D, Rattei T, Mewes HW, Wagner M (2004) Illuminating the evolutionary history of chlamydiae. Science 304(5671): 728–730

Kebbi-Beghdadi C, Batista C, Greub G (2011a) Permissivity of fish cell lines to three Chlamydia-related bacteria: *Waddlia chondrophila*, *Estrella lausannensis* and *Parachlamydia acanthamoebae*. FEMS Immunol Med Microbiol 63(3):339–345. doi:10.1111/j.1574-695X.2011.00856.x

Kebbi-Beghdadi C, Cisse O, Greub G (2011b) Permissivity of Vero cells, human pneumocytes and human endometrial cells to *Waddlia chondrophila*. Microbes Infect 13(6): 566–574

Labutti K, Sikorski J, Schneider S, Nolan M, Lucas S, Glavina Del Rio T, Tice H, Cheng JF, Goodwin L, Pitluck S, Liolios K, Ivanova N, Mavromatis K, Mikhailova N, Pati A, Chen A, Palaniappan K, Land M, Hauser L, Chang YJ, Jeffries CD, Tindall BJ, Rohde M, Goker M, Woyke T, Bristow J, Eisen JA, Markowitz V, Hugenholtz P, Kyrpides NC, Klenk HP, Lapidus A (2010) Complete genome sequence of *Planctomyces limnophilus* type strain (Mu 290). Stand Genomic Sci 3(1):47–56

Lee KC, Webb RI, Janssen PH, Sangwan P, Romeo T, Staley JT, Fuerst JA (2009) Phylum Verrucomicrobia representatives share a compartmentalized cell plan with members of bacterial phylum Planctomycetes. BMC Microbiol 9:5. doi:10.1186/1471-2180-9-5

Lienard J, Greub G (2011) Discovering new pathogens: amoebae as tools to isolate amoeba-resisting microorganisms from environmental samples. In: Sen K, Ashbolt NJ (eds) Environmental microbiology: current technology and water applications. Caister Academic Press, Norfolk, p 143e162

Lienard J, Croxatto A, Prod'hom G, Greub G (2011) *Estrella lausannensis*, a new star in the *Chlamydiales* order. Microbes Infect 13:1232–1241

Lindsay MRW, Webb RI, Hosmer HM, Fuerst JA (1995) Effects of fixative and buffer on morphology and ultrastructure of a freshwater planctomycete, *Gemmata obscuriglobus*. J Microbiol Methods 21:45–54

Matsumoto A, Fujiwara E, Higashi N (1976) Observations of the surface projections of infectious small cell of *Chlamydia psittaci* in thin sections. J Electron Microsc 25(3):169–170

McCoy AJ, Maurelli AT (2006) Building the invisible wall: updating the chlamydial peptidoglycan anomaly. Trends Microbiol 14(2):70–77. doi:10.1016/j.tim.2005.12.004

Mitchell CM, Mathews SA, Theodoropoulos C, Timms P (2009) In vitro characterisation of koala *Chlamydia pneumoniae*: morphology, inclusion development and doubling time.

Vet Microbiol 136(1–2):91–99. doi:10.1016/j.vetmic.2008.10.008

Miyashita N, Matsumoto A, Fukano H, Niki Y, Matsushima T (2001) The 7.5-kb common plasmid is unrelated to the drug susceptibility of *Chlamydia trachomatis*. J Infect Chemother 7(2):113–116. doi:10.1007/s1015610070113

Rasband WS (1997–2012) ImageJ. U. S. National Institutes of Health, Bethesda

RCoreTeam (2012) R: a language and environment for statistical computing. R foundation for statistical computing, Vienna

Schneider CA, Rasband WS, Eliceiri KW (2012) NIH Image to ImageJ: 25 years of image analysis. Nat Methods 9(7):671–675

Staley JT (1968) Prosthecomicrobium and Ancalomicrobium: new prosthecate freshwater bacteria. J Bacteriol 95(5):1921–1942

Stephens RS, Kalman S, Lammel C, Fan J, Marathe R, Aravind L, Mitchell W, Olinger L, Tatusov RL, Zhao Q, Koonin EV, Davis RW (1998) Genome sequence of an obligate intracellular pathogen of humans: *Chlamydia trachomatis*. Science 282(5389):754–759

Thomas V, Casson N, Greub G (2006) *Criblamydia sequanensis*, a new intracellular Chlamydiales isolated from Seine river water using amoebal co-culture. Environ Microbiol 8(12):2125–2135

Venables WN, Ripley BD (2002) Modern applied statistics with S, 4th edn. Springer, New York

Yoon J, Matsuo Y, Matsuda S, Kasai H, Yokota A (2010) *Cerasicoccus maritimus* sp. nov. and *Cerasicoccus frondis* sp. nov., two peptidoglycan-less marine verrucomicrobial species, and description of Verrucomicrobia phyl. nov., nom. rev. J Gen Appl Microbiol 56(3):213–222